Joule

CellPress

Article

Efficiency Limits of Underwater Solar Cells

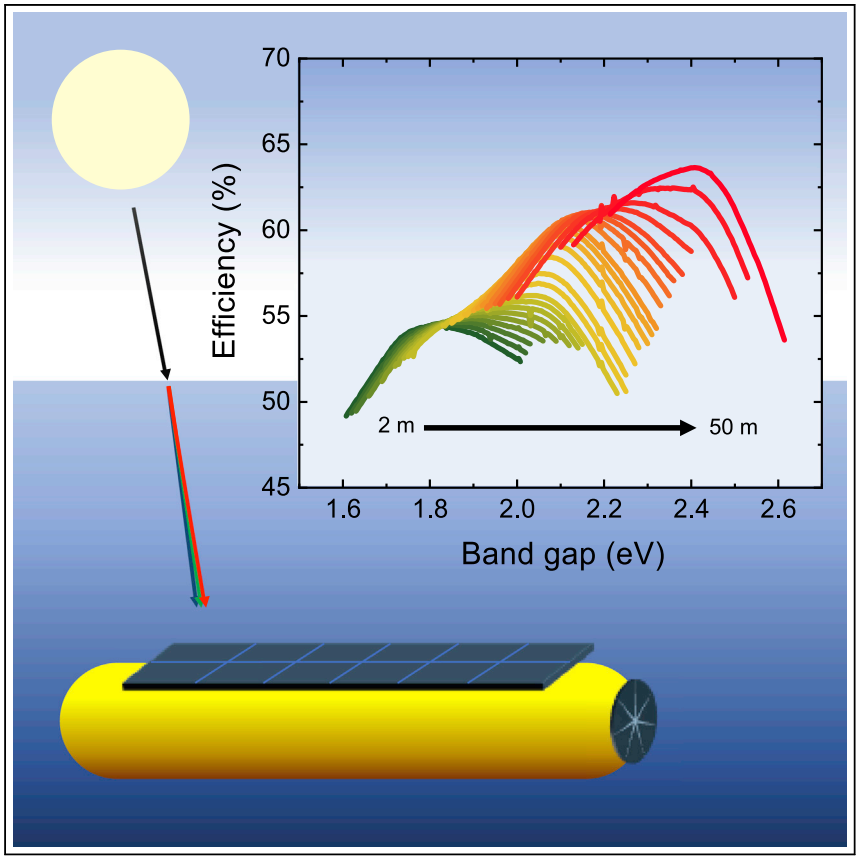

Most attempts to use solar cells to power underwater systems have had limited success due to the use of materials with relatively narrow band gaps such as silicon. We performed detailed balance calculations combined with oceanographic data to show that, if wide-band-gap semiconductors are employed, underwater solar cells can operate at efficiencies up to ~65% while still generating useful power. Finally, we propose both organic and inorganic materials that could be used to maximize underwater power generation and efficiency.

Jason A. Röhr, Jason Lipton, Jaemin Kong, Stephen A. Maclean, André D. Taylor

adt4@nyu.edu

HIGHLIGHTS

Underwater cells can produce useful power at up to 65% efficiency in clearest waters

The optimum band gap of the solar cell plateaus at ~2.1 eV at intermediate depths

Band-gap values are relatively independent of geographical location

Röhr et al., Joule 4, 840–849
April 15, 2020
https://doi.org/10.1016/j.joule.2020.02.005

Joule

CellPress

Article

Efficiency Limits of Underwater Solar Cells

Jason A. Röhr,[1] Jason Lipton,[1] Jaemin Kong,[1] Stephen A. Maclean,[1] and André D. Taylor[1,2,*]

SUMMARY

Operation of underwater vehicles and autonomous systems is currently limited by the lack of long-lasting power sources. These systems could potentially be powered using underwater solar cells, but the material requirements to achieve their full potential are not well understood. Using detailed-balance calculations, we show that underwater solar cells can exhibit efficiencies from ~55% in shallow waters to more than 65% in deep waters, while maintaining a power density >5 mW cm^{-2}. We show that the optimum band gap of the solar cell shifts by ~0.6 eV between shallow and deep waters and plateaus at ~2.1 eV at intermediate depths, independent of geographical location. This wide range in optimum band-gap energies opens the potential for a library of wide-band-gap semiconductors to be used for high-efficiency underwater solar cells. Our results provide a roadmap for proper choice of underwater solar cell materials, given the conditions at points of use.

INTRODUCTION

Long-term operation of underwater vehicles, autonomous systems, and sensors is severely limited by the lack of enduring power sources and typically rely on on-shore power, on-board batteries, or power from solar cells situated above water or on land.[1–3] Where solar cells have proven to be a viable technology for powering both land- and space-based devices,[4] directly using underwater solar cells to power marine systems has only briefly been considered.[3,5,6] Previous attempts to use underwater solar cells to run autonomous systems have had limited success due to the use of solar cells made from silicon (Si) or amorphous Si (a-Si), which have band gaps of ~1.11 and ~1.8 eV, respectively, and are optimized to function on land.[7,8] Water both scatters and absorbs visible light, with a large amount of the red part of the solar spectrum (>600 nm) being absorbed at shallow depths. In fact, the blue to yellow part of the spectrum (400–600 nm) is the last portion to be absorbed, and thus penetrates the farthest below the surface.[9] The underwater spectrum is for that reason biased toward using wider band-gap semiconductors for solar cells (≥1.8 eV), thus traditional solar cells that employ narrow-band-gap semiconductors are not optimal for deep-water applications.

Besides a-Si, a few other wide-band-gap semiconductors have been investigated for underwater solar cells. Jenkins et al. showed that InGaP solar cells, with a band gap of around 1.8 eV, could efficiently harvest solar energy yielding useful power at depths as great as 9 m below sea level.[3,10] However, the cost of InGaP solar cells has so far been a hindrance in adoption of the technology, though recent advances in the growth of III-V semiconductors have shown that costs can be greatly reduced.[11] Organic photovoltaic systems, utilizing wide-band-gap semiconducting polymers and small molecules, have also briefly been studied by both Jenkins and co-workers[5] and Kong et al.[12] Organic semiconductors have been shown to function

Context & Scale

Most attempts to use solar cells to power underwater systems have had limited success due to the use of silicon, which has a relatively narrow band gap and absorbs ultraviolet (UV), visible, and infrared (IR) light. Because of absorption by water, most of the IR light from the sun is absorbed at relatively shallow depths, and wider band-gap semiconductors, which primarily absorb visible light, should therefore be used. To understand how efficient underwater solar cells can be and what band gaps are optimum in deep waters, we combined oceanographic data with detailed balance calculations to show that solar cells can harvest useful power at water depths down to 50 m with very high efficiencies. Our findings show that underwater solar cells can efficiently generate useful power in very deep waters but should employ much wider band-gap semiconductors than what are currently used today.

more efficiently under low-lighting conditions, making them optimal for underwater solar cells.[13] Besides the already investigated systems, a large number of organic and inorganic wide-band-gap semiconductors exist that are currently not being considered for solar cell applications due to their band gaps being too large for land-based applications. These semiconductors could, however, be highly useful for underwater applications.

Detailed-balance analysis has previously been used to determine the ultimate efficiency limits of land- and space-based solar cells. Shockley and Queisser famously used detailed-balance analysis to show that the maximum efficiency that can be obtained from a land-based solar cell is ~34% (the so-called Shockley-Queisser limit);[14] however, when the irradiance spectrum is narrowed, the maximum efficiency limits increase.[15] As such, detailed balance calculations have also been used to estimate the theoretical efficiency maxima of indoor solar cells when illuminated with various light sources with narrow emission spectra, where it was shown that solar cells can operate at efficiencies of ~60% when illuminated by light-emitting diodes (LEDs) and ~67% when illuminated by sodium discharge lamps.[16] A similar narrowing of the irradiance spectrum is observed when light is transmitted through water,[3] and we therefore expect profound increases in the efficiency limits of underwater solar cells.

In this study, we conduct detailed-balance calculations to show the ultimate potential of underwater solar cells. We show that in the Earth's clearest natural waters, solar cells can harvest useful power from the sun at depths down to 50 m below sea level with efficiencies ranging from ~55% at 2 m to more than 63% at 50 m. An additional boost in efficiency can be achieved when the solar cells are operated in cold waters. We show that the optimum band gap of the solar cell absorber shifts from ~1.8 eV when operated at 2 m to ~2.4 eV at 50 m, with a band-gap plateau at ~2.1 eV between 4 and 20 m. We also show that the optimum band-gap values are more or less independent of which waters the solar cell is deployed in, which is highly beneficial from a design perspective, as the solar cells would not have to be tailored to specific waters but rather to specific operating depths. Our findings open up the potential for the large library of currently overlooked wide-band-gap semiconductors, both organic and inorganic, to be used as absorbers for high-efficiency underwater solar cell applications.

RESULTS AND DISCUSSION

Representative Water Spectra

To assess the potential of underwater solar cells as a useful technology, a range of waters of varying clarity, ranging from the clearest waters found in the Pacific and Atlantic oceans to more turbid lake water found in Finland, were assessed. For comparison, spectra for deionized (DI) water were also considered. The spectra were specifically chosen from more than 400 published spectra to investigate waters with highly varied absorption characteristics, both in shape and overall magnitude. The most turbid waters assessed in this study are by no means the least clear waters found on Earth. Rather, we only assess waters that are clear enough to support solar cells and still yield useful power of 5 mW cm^{-2}.[3]

The absorption coefficient of pure DI water has been published on several occasions. Where most measurements agree from the green part of the spectral range to the near IR (>450 nm), differences are commonly reported in the UV to blue part of the spectrum (300–450 nm) due to low absorption by water in those regions, making accurate measurements difficult. Out of the many published spectra, we consider

[1]Tandon School of Engineering, Department of Chemical and Biomolecular Engineering, New York University, Brooklyn, New York, NY 11201, USA

[2]Lead Contact

*Correspondence: adt4@nyu.edu

https://doi.org/10.1016/j.joule.2020.02.005

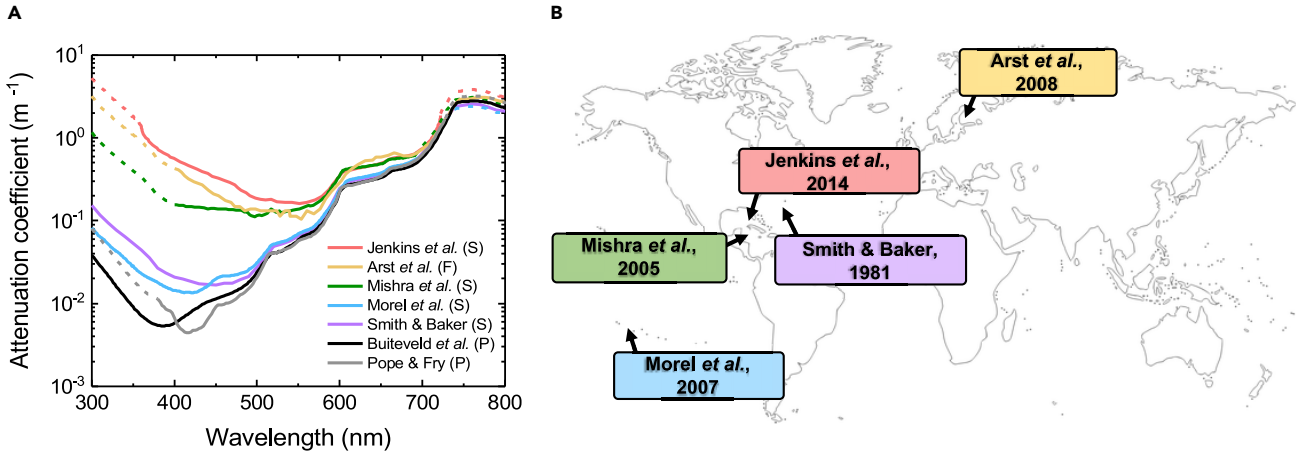

Figure 1. Water Absorption Profiles at Various Locations on Earth

(A) Attenuation spectra, either absorption spectra or diffuse attenuation coefficients of selected saltwater (S), fresh (F), and pure DI water (P).

(B) World map showing where the selected water spectra were acquired: waters in the South Pacific (Morel et al.),[19] off the coast of Roatan Island in Honduras (Mishra et al.),[20] off the coast of Key West, Florida, in the United States (Jenkins et al.),[3] waters from the Sargasso Sea (Smith and Baker),[21] and waters from lake Äntu Sinijärv in Finland (Arst et al.).[22]

It should be noted that the spectrum by Pope and Fry[18] was not recorded from 300 to 380 nm and the spectrum by Buiteveld et al.[17] was used to extend the spectrum. Similarly, the spectra by Jenkins et al.,[3] Morel et al.,[19] Mishra et al.,[20] and Arst et al.[22] were extended using the full spectrum by Smith and Baker.[21] All extensions are shown as dashed lines.

the spectra by Buiteveld et al.[17] and Pope and Fry[18] (Figure 1A), which have been cited as some of the most reliable. Whereas absorption spectra for pure water have been published, sea and lake water transparency metrics are usually classified by their diffuse attenuation coefficients, which is the combined absorption and scattering coefficient and hence the most relevant for consideration of underwater solar cells. Diffuse attenuation coefficient spectra obtained from oceanic waters off the coast of Key West (Jenkins et al.),[3] waters in the South Pacific (Morel et al.),[19] waters close to Roatan Island in Honduras (Mishra et al.),[20] and waters from the Sargasso Sea (Smith and Baker),[21] along with a spectrum from lake Äntu Sinijärv in Finland (Arst et al.),[22] were used for the feasibility analysis (Figure 1A).

Similarities exist between all the considered absorption and attenuation spectra. Most noteworthy, both the spectra for pure water and the spectra for sea and lake water transmit almost equally between 600 and 800 nm, with turbid water having a slightly lower transmission of red and IR light. From the UV to visible light, the clearest waters are highly transmissive, with the turbid waters absorbing most of the UV light. As will be clear from the detailed-balance analysis below, both the shape and overall magnitude of the water spectra have profound implications on the efficiency limits and the optimum band gaps of the solar cells.

Underwater Solar Cell Efficiency Limits

Since all the attenuation spectra shown in Figure 1A absorb a near equal amount of light from 600 to 800 nm, light between 700 and 800 nm is almost fully absorbed at shallow depths ($D = 2$ m) regardless of the examined water (Figures 2A–2C). Light at wavelengths larger than 700 nm will therefore not contribute toward useful power; however, significant differences between the attenuation spectra are observed when comparing the transmitted light at wavelengths smaller than 600 nm (Figures 2A–2C). The water in the South Pacific (Morel et al.)[19] attenuates significantly less UV and blue light than the water in Key West (Jenkins et al.).[3] Because the solar cell is evaluated under water, these differences in transmitted light have significant

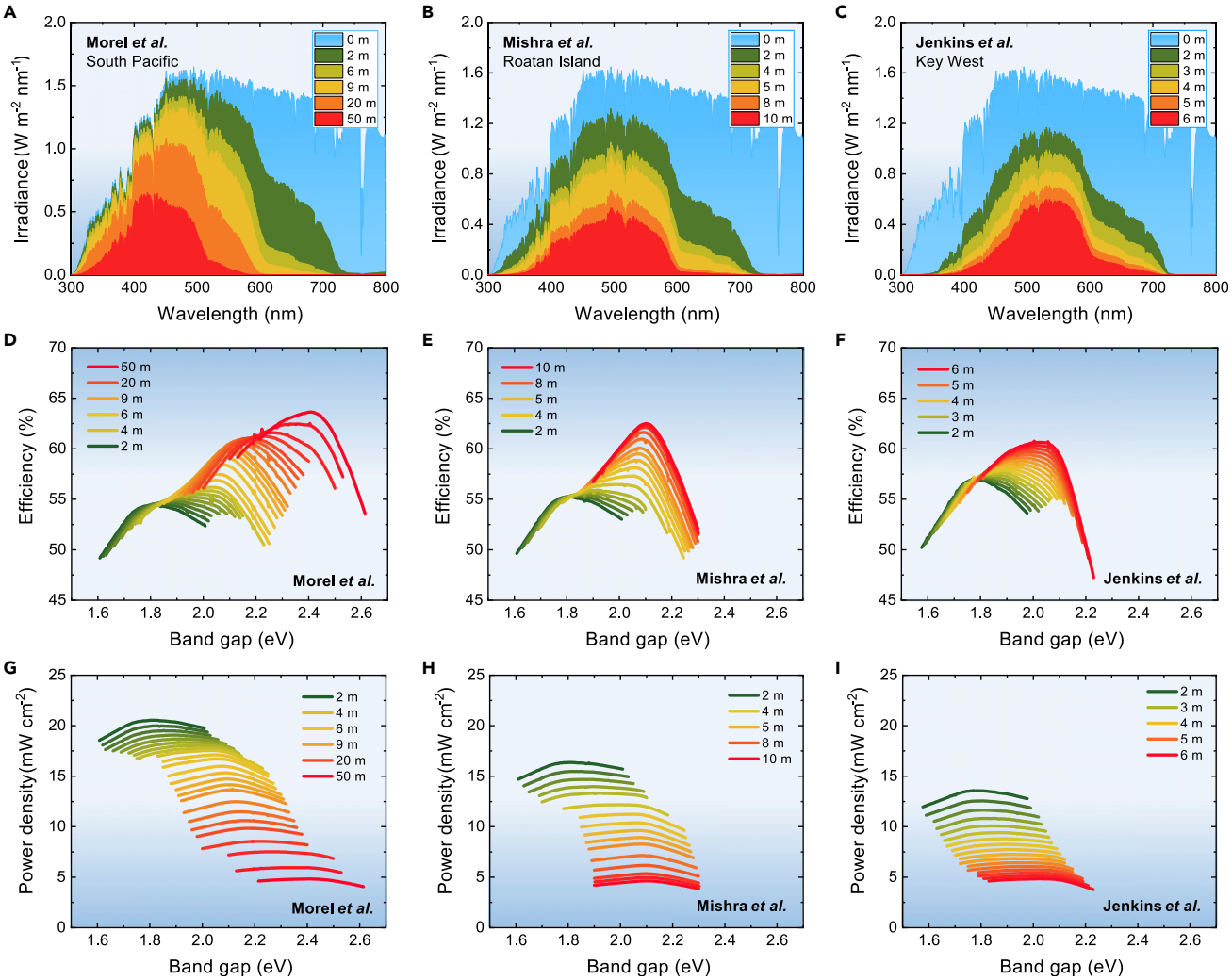

Figure 2. Detailed-Balance Results for Underwater Solar Cells at Three Different Locations

(A–C) Changes in the solar spectrum at various water depths at three different locations with attenuation spectra varying in both shape and magnitude: South Pacific (Morel et al.),[19] off the coast of Roatan Island (Mishra et al.),[20] and lake Äntu Sinijärv (Arst et al.).[22]

(D–F) Efficiency as a function of examined band gap at various depths.

(G–I) Power density as a function of examined band gap. The depth was increased during the calculations until a power density of 5 mW cm^{-2} was reached.

All calculations were performed at 300 K to allow for a direct comparison with the Shockley-Queisser limit.

implications for how efficiently the solar cell can generate power, the magnitude of the power density, and the value for the optimum band gap.

We utilized an idealized detailed-balance model to assess the ultimate efficiency limits for underwater solar cells.[14,23] The model assumes a step function for the semiconductor absorption edge and that charge carriers are only lost via unavoidable radiative recombination. Non-radiative recombination, which is usually observed in many organic and inorganic solar cells, is, therefore, not considered directly.[24–26] When evaluated at the surface, the detailed balance model yields the classical Shockley-Queisser limit with optimum band-gap values between ~ 1.1 and ~ 1.4 eV and a maximum efficiency of ~ 33% (Figure S1A).[14] As surface waves affect the incoming spectrum just below sea level depending on the weather,[3] the generated power density and efficiency of the underwater solar cells were

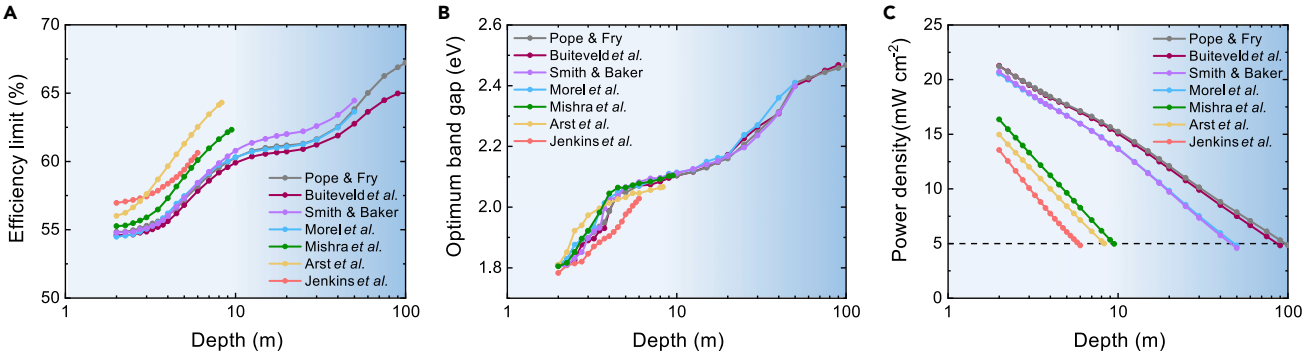

Figure 3. Detailed-Balance Results for All Investigated Waters as a Function of Operation Depth

(A) Solar cell efficiency limits.

(B) Optimum semiconductor band gaps.

(C) Maximum power density above 5 mW cm^{-2} as a function of depth.

All calculations were performed at 300 K.

investigated from 2 m below sea level down to a maximum of 100 m. In order to make a direct comparison with the Shockley-Queisser limit, all calculations were performed at room temperature (300 K) unless otherwise noted. The effect of changing the temperature to more realistic values is subsequently discussed.

The calculated efficiencies and power densities as a function of band gap, when the irradiance spectrum is modified using the water attenuation spectra, are shown in Figures 2D–2F and 2G–2I, respectively. The least attenuating water (Morel et al.)[19] allows for harvesting of a power density greater than 5 mW cm^{-2} up to a depth of 50 m below sea level (Figure 2G). The maximum efficiency is seen to increase from ~ 54% up to ~ 63% going from a depth of 2 to 50 m (Figure 2D). Two efficiency maxima plateaus are observed, which are due to the similar plateaus observed in the red and IR parts of the attenuation spectra since light above 600 nm is absorbed by a much greater amount (Figure 1A). A similar plateau is observed in Figure 2E (Mishra et al.),[20] though the second plateau is not observed because of the overall increase of the absorptive properties of the water. No plateau is observed in Figure 2F because UV and IR light are similarly attenuated. The variation of the power densities between the different spectra at various water depths are shown in Figures 2G–2I.

The large increase of the solar cell efficiency beyond the Shockley-Queisser limit, even in shallow waters (2 m), is due to the narrowing of the transmitted solar spectrum reaching the solar cell. The high degree of attenuated IR and red light and the high transmittance of UV to green light (as shown in the spectrum published by Morel et al.[19] in Figure 2A) results in a narrow transmitted irradiance spectrum between 300 and 500 nm (with a small amount of transmitted light between 500 and 600 nm). This gives rise to a maximum efficiency of ~ 63% for a solar cell with a band gap of 2.4 eV at a depth of 50 m (Figures 2A and 2D). For the spectrum by Mishra et al.,[20] a similar narrowing is observed, yielding an irradiance spectrum between 400 and 600 nm, giving a maximum efficiency of ~ 62.5% with a band gap of 2.1 eV at a depth of 10 m. For the spectrum by Jenkins et al.,[3] the transmitted irradiance spectrum has a significant contribution between 600 and 700 nm, giving a slightly lower (but still high) efficiency limit of ~ 61% at a band gap of around 2.05 eV. An even higher efficiency (~ 67%) can be obtained for pure DI water (Pope and Fry)[18] at a depth of 100 m (Figure S2). Efficiency limits, for all of the considered water spectra, are shown in Figure 3A. It should be noted that while non-radiative

recombination was not included into the calculations due to the reduction in both short-circuit current and open-circuit voltage caused by the loss of charge carriers, an even greater increase in the optimum band gap is expected (along with a reduction in the overall efficiency limit). However, as discussed in the following section, materials do exist that operate very close to their radiative limits.

The World's oceans are highly complex physicochemical systems and water temperatures can vary greatly, typically decreasing at large depths.[27] Because of the decrease in radiative recombination with decreased temperature, a slight increase in efficiency can be obtained when the solar cell is operated in cold waters. For example, the Shockley-Queisser limit increases by 3.4%–4.3% when operated at 272.15 K compared to 300 K (Figures S1A and S1B). This is a 8.1%–10.2% increase over the efficiency of the cell at operating temperatures of 338.15 K.[28] Similar to what is observed for terrestrial solar cells, an increase in efficiency (~2.4%) between a solar cell operated at 300 and 272.15 K can be obtained for the waters in the South Pacific (Morel et al.),[19] as shown in Figure S3. This increase is an added bonus arising simply from the operating conditions, which also reduces the need for heat management.[28] Additionally, differences in refractive index at the air/water interface cause the light to focus downward into the water and onto the cell, reducing the need for automated solar tracking, with an increase in the focusing effect in the blue to UV part of the spectrum (Figure S4).[8]

Potential Semiconductor Candidates

Regardless of the investigated water, the requirement for the semiconductor band gap is surprisingly similar (Figure 3B). In shallow waters (2–4 m), the optimum band gap shifts from ~1.8 to ~2.1 eV in all cases. A band-gap plateau is then observed at a value of ~2.1 eV until a depth of 20 m. At larger depths, the optimum band gap shifts to large values, eventually reaching values >2.4 eV (the solar cell is generating power in excess of 5 mW cm^{-2} for all cases, as shown in Figure 3C). The fact that the optimum band-gap values are more or less independent of which waters the solar cell is deployed in is highly beneficial from a design perspective since the solar cells would not have to be tailored to specific waters but rather to specific operating depths.

Many direct inorganic and organic wide-band-gap semiconductors exist that could be considered for high-efficiency underwater solar cells. As an example, the band gap of hydrogenated a-Si (a-Si:H) can be tuned between 1.55 to 2.1 eV, which makes it an ideal candidate for operation at a depth down to 10 m.[29] a-Si cells have already been considered for underwater applications but tuning the band gap to a larger value is necessary for optimum performance. Semiconductors such as CuO_2 and ZnTe have even larger band gaps of 2.17 and 2.25 eV, making them potential candidates for operation at depths of 20 and 30 m, respectively;[30,31] however, defects and film quality is currently limiting the terrestrial efficiency of CuO_2 to around 6%[32] and ZnTe for solar cell applications is relatively unexplored.[33]

Ternary and quaternary compound semiconductors such as cadmium zinc telluride (CZT),[31] cupper zinc antimony sulfide (CZAS),[34] AlGaAs,[35] InGaP,[3,36] and GaAsP[37] have tunable band gaps and can therefore be tailored to perform at various depths. Certain III-V semiconductor solar cells can operate very close to the radiative limit,[38] and it is therefore likely that III-V-based solar cells have the highest potential to reach their ultimate efficiency limits, making AlGaAs, InGaP, and GaAsP excellent candidates for underwater solar cells. III-V semiconductor solar cells are typically deemed to be too expensive for mass production due to the need of single-crystal substrates

and epitaxial growth;[6] however, it was recently shown that these compound materials can be grown with inexpensive techniques, severely decreasing the fabrication costs.[11]

Organic solar cells also have the potential to be low cost and have been shown to work more efficiently under low-light conditions.[13] Organic solar cells are excitonic solar cells, which means that they rely on donor-acceptor interfaces that ultimately reduces the efficiency limit due to a reduced open-circuit voltage;[39] however, organic solar cells are lightweight and can be made flexible, allowing for easy integration with underwater systems without adding much weight or bulk.[40] Poly(3-hexylthiophene-2,5-diyl) (P3HT) is widely considered to be one of the most scalable polymeric semiconductors.[41] With a band gap of ~1.9 eV, P3HT is not ideal for high-efficiency land-based solar cells but could be a perfect candidate for operation in shallow waters.[5,12] Other wide-band-gap organic semiconductors have been developed for light-emitting diodes and field-effect transistors. Candidates for deep-water underwater solar cells could therefore potentially be found among the materials used for these technologies. For example, materials such as rubrene (2.2 eV) and pentacene (2.2 eV) could be good candidates,[42–44] and for solar cells operated at large depths, poly(*p*-phenylene vinylene) derivatives (2.3–2.4 eV) could be ideal organic semiconductor materials.[45,46]

With the recent development of replacing fullerenes with non-fullerene acceptors to achieve both greater performing organic solar cells and improved device stability,[47–49] a number of new wide-band-gap semiconductor donor materials have been developed, yielding higher efficiencies than traditional systems that were paired with fullerene derivatives. For example, the polymers PFBDB-T (~2.04 eV), PDTB-EF-T (~1.93 eV), and PM6 (~1.97 eV) were paired with non-fullerene acceptors to yield efficiencies of ~12.4%, ~14.2%, and ~15.7%, respectively.[50–52] While these wide-band-gap materials yielded excellent efficiencies for land-based solar cells, even wider band-gap donor materials should be synthesized for both shallow and deep-sea applications. These new donor materials should then be paired with optimum acceptors to maximize both the efficiency and power generation.

Finally, an important consideration is the solar cell material's stability in maritime environments. It has been shown that unmodified, encapsulated Si solar panels, can stay submerged underwater during operation for months without any significant loss in power conversion efficiency.[53] While Si is not optimum for deep-sea applications, similar encapsulation techniques could be employed to stabilize solar cells made from wide-band-gap semiconductors. For organic solar cells, water tends to negatively affect charge transport in organic semiconductors,[54] so proper encapsulation methods must therefore be employed.[55] Alternatively, we have recently demonstrated that organic solar cells can be made resilient to water by selectively removing the acceptor material from the top surface,[12] allowing for a dual-safeguarding strategy.

Conclusions

The results presented herein provide a foundation for determining proper choice of solar cell materials for use in underwater applications. Using detailed-balance calculations, we show that underwater solar cells have the potential to harvest useful power at depths down to 50 m with efficiencies ranging from ~55% in shallow waters to more than 65% in deep waters, all while generating power greater than 5 mW cm^{-2}. We find that the optimum band gap of the absorbing semiconductor depends mainly on water depth and less on the geographic location where the solar cell is deployed. Our calculations show that the optimum band gap of the solar

cell shifts from ~1.8 to ~2.4 eV between shallow and deep waters, with a band-gap plateau at ~2.1 eV between 4 and 20 m. The fact that the optimum band gap mainly depends on water depth is highly beneficial from a device design perspective since the solar cells would not have to be tailored to specific waters but could rather be tailored to operate at specific depths. Since wide-band-gap semiconductors are not conventionally desired for outdoor solar harvesting, the large library of inorganic and organic wide-band-gap semiconductors, currently not considered for land-based solar cells, could potentially be used as absorbers in high-efficiency underwater solar cells.

EXPERIMENTAL PROCEDURES

The power conversion efficiency of a solar cell, η, is given by the ratio of the power density output, p_{out}, to the power density input from the solar spectrum, p_{in}:

$$\eta = \frac{p_{out}}{p_{in}}. \quad \text{(Equation 1)}$$

The output power can be measured from the maximum power point of the solar cell *J-V* curve, $p_{out} = J_{max}V_{max}$, and p_{in} is measured by integrating the photon flux density, i.e., the number of photons hitting the surface per unit time:

$$p_{in}(D) = \int_{-\infty}^{\infty} \Phi_D(E, D)dE \quad \text{(Equation 2)}$$

where, $\Phi_D(E, D)$ is the water absorption-corrected photon flux density, E is the photon energy, and D is the depth below sea level. $\Phi_D(E, D)$ is related to the wavelength-dependent AM1.5G spectral irradiance spectrum by:

$$\Phi_D(E, D) = \varphi_{AM1.5G}(\lambda)\exp\{-\alpha_D(\lambda)D\}\frac{hc}{E^2} \quad \text{(Equation 3)}$$

where the exponential term is a Beer-Lambert correction to the spectral irradiance due to light absorption by the water, α_D (Figures 2A–2C). Assuming that each photon with energy $\hbar\omega > E_g$, where E_g is the band-gap energy of the semiconductor, contributes to one electron-hole pair, the photocurrent density can be defined via the photon flux density:

$$J_{ph}(E_g, D) = q\int_{E_g}^{\infty} \Phi_D(E, D)E^{-1}dE. \quad \text{(Equation 4)}$$

Radiative recombination is inevitable for any body of matter with a temperature >0 K. Assuming ideal diode behavior and that the quasi-Fermi level splitting is equal to the external voltage, V, the lowest possible radiative recombination current density can be described by:

$$J_{rec}(V, E_g, T_c) = \frac{2\pi q}{c^2h^3}\int_{E_g}^{\infty} \frac{E^2}{\exp\left(\frac{E - qV}{k_B T_c}\right) - 1}dE. \quad \text{(Equation 5)}$$

Since total current density is only due to electrons and holes that have not recombined,

$J = J_{ph} - J_{rec}$, the solar cell *J-V* curve can be described by:

$$J(V, E_g, D, T_c) = q\left(\int_{E_g}^{\infty} \Phi_D(E, D)E^{-1}dE - \frac{2\pi}{c^2h^3}\int_{E_g}^{\infty} \frac{E^2}{\exp\left(\frac{E - qV}{k_B T_c}\right) - 1}dE\right) \quad \text{(Equation 6)}$$

For a given absorption spectrum, and for given values of E_g, D, and T_c, the detailed-balance efficiency limit can be obtained by evaluating Equations 1 and 2 and maximizing the JV product in Equation 6 to obtain $J_{max}V_{max}$.

DATA AND CODE AVAILABILITY

All data that support the findings in this study are present in the paper and in the Supplemental Information. Data are available from the corresponding author upon reasonable request.

SUPPLEMENTAL INFORMATION

Supplemental Information can be found online at https://doi.org/10.1016/j.joule.2020.02.005.

ACKNOWLEDGMENTS

The authors want to thank Mr. Hang Wang for fruitful discussions and Dr. Steven J. Byrnes for writing the foundation code (available at https://sjbyrnes.com/). The authors gratefully acknowledge funding support from New York University. This paper is dedicated to the memory of Dr. Phillip Pierce Jenkins, a pioneer of underwater solar cells, whose work is a source of great inspiration.

AUTHOR CONTRIBUTIONS

Conceptualization, J.A.R.; Methodology, J.A.R.; Software, J.A.R.; Investigation, J.A.R., J.L., and J.K., Resources, J.L. and S.A.M.; Writing – Original Draft, J.A.R.; Writing – Review and Editing, J.A.R., J.L., J.K., S.A.M., and A.D.T.; Visualization, J.A.R.; Supervision, A.D.T.

DECLARATION OF INTERESTS

The authors declare no competing interests.

Received: November 19, 2019
Revised: January 14, 2020
Accepted: February 17, 2020
Published: March 18, 2020

REFERENCES

1. Crimmins, D.M., Patty, C.T., Beliard, M.A., Baker, J., Jalbert, J.C., Komerska, R.J., Chappell, S.G., and Blidberg, D.R. (2006). Long-endurance test results of the solar-powered AUV system. In Oceans 2006 (IEEE), pp. 1–5.

2. Wang, X., Shang, J., Luo, Z., Tang, L., Zhang, X., and Li, J. (2012). Reviews of power systems and environmental energy conversion for unmanned underwater vehicles. Renew. Sustain. Energy Rev. *16*, 1958–1970.

3. Jenkins, P.P., Messenger, S., Trautz, K.M., Maximenko, S.I., Goldstein, D., Scheiman, D., Hoheisel, R., and Walters, R.J. (2014). High-bandgap solar cells for underwater photovoltaic applications. IEEE J. Photovoltaics *4*, 202–207.

4. Nelson, J. (2003). The Physics of Solar Cells (Imperial College Press).

5. Walters, R.J., Yoon, W., Placencia, D., Scheiman, D., Lumb, M.P., Strang, A., Stavrinou, P.N., and Jenkins, P.P. (2015). Multijunction organic photovoltaic cells for underwater solar 2015 IEEE 42nd Photovoltaic Specialist Conference (PVSC), pp. 1–3.

6. Jenkins, P., and Walters, R. (2017). Photovoltaic technology for navy and marine corps applications. 2017 IEEE 60th International Midwest Symposium on Circuits and Systems (MWSCAS), 958–961.

7. Arima, M., Okashima, T., and Yamada, T. (2011). Development of a solar-powered underwater glider. IEEE Symposium on Underwater Technology and Workshop on Scientific Use of Submarine Cables and Related Technologies, pp. 1–5.

8. Joshi, K.B., Costello, J.H., and Priya, S. (2011). Estimation of solar energy harvested for autonomous jellyfish vehicles (AJVs). IEEE J. Oceanic Eng. *36*, 539–551.

9. Stachiw, J.D. (1980). Performance of photovoltaic cells in an undersea environment. J. Eng. Ind. *102*, 51–59.

10. Notman, N. (2012). Underwater solar cells. Mater. Today *15*, 301.

11. Simon, J., Schulte, K.L., Horowitz, K.A.W., Remo, T., Young, D.L., and Ptak, A.J. (2019). III-V-based optoelectronics with low-cost dynamic hydride vapor phase epitaxy. Crystals *9*, 1–14.

12. Kong, J., Nordlund, D., Jin, J.S., Kim, S.Y., Jin, S.-M., Huang, D., Zheng, Y., Karpovich, C., Sertic, G., Wang, H., et al. (2019). Underwater organic solar cells via selective removal of electron acceptors near the top electrode. ACS Energy Lett. *4*, 1034–1041.

13. Steim, R., Ameri, T., Schilinsky, P., Waldauf, C., Dennler, G., Scharber, M., and Brabec, C.J. (2011). Organic photovoltaics for low light applications. Sol. Energy Mater. Sol. Cells *95*, 3256–3261.

14. Shockley, W., and Queisser, H.J. (1961). Detailed balance limit of efficiency of p-n junction solar cells. J. Appl. Phys. *32*, 510–519.

15. Bahrami-Yekta, V., and Tiedje, T. (2018). Limiting efficiency of indoor silicon photovoltaic devices. Opt. Express *26*, 28238–28248.

16. Freunek, M., Freunek, M., and Reindl, L.M. (2013). Maximum efficiencies of indoor photovoltaic devices. IEEE J. Photovoltaics *3*, 59–64.

17. Buiteveld, H., Hakvoort, J.H.M., and Donze, M. (1994). Optical properties of pure water. SPIE Proc. Ocean Optics XII *2258*, 174–183.

18. Pope, R.M., and Fry, E.S. (1997). Absorption spectrum (380–700 nm) of pure water. II. integrating cavity measurements. Appl. Opt. *36*, 8710–8723.

19. Morel, A., Gentili, B., Claustre, H., Babin, M., Bricaud, A., Ras, J., and Tièche, F. (2007). Optical properties of the "clearest" natural waters. Limnol. Oceanogr. *52*, 217–229.

20. Mishra, D.R., Narumalani, S., Rundquist, D., and Lawson, M. (2005). Characterizing the vertical diffuse attenuation coefficient for downwelling irradiance in coastal waters: implications for water penetration by high resolution satellite data. ISPRS J. Photogramm. *60*, 48–64.

21. Smith, R.C., and Baker, K.S. (1981). Optical properties of the clearest natural waters (200–800 nm). Appl. Opt. *20*, 177–184.

22. Arst, H., Erm, A., Herlevi, A., Kutser, T., Leppäranta, M., Reinart, A., and Virta, J. (2008). Optical properties of boreal lake waters in Finland and Estonia. Boreal Environ. Res. *13*, 133–158.

23. Guillemoles, J.-F., Kirchartz, T., Cahen, D., and Rau, U. (2019). Guide for the perplexed to the Shockley–Queisser model for solar cells. Nat. Photonics *13*, 501–505.

24. Kirchartz, T., Mattheis, J., and Rau, U. (2008). Detailed balance theory of excitonic and bulk heterojunction solar cells. Phys. Rev. B *78*, 1–13.

25. Rau, U., Paetzold, U.W., and Kirchartz, T. (2014). Thermodynamics of light management in photovoltaic devices. Phys. Rev. B *90*, 1–16.

26. Azzouzi, M., Cabas-Vidani, A., Haass, S.G., Röhr, J.A., Romanyuk, Y.E., Tiwari, A.N., and Nelson, J. (2019). Analysis of the voltage losses in CZTSSe solar cells of varying Sn content. J. Phys. Chem. Lett. *10*, 2829–2835.

27. Schorstein, K., Fry, E.S., and Walther, T. (2009). Depth-resolved temperature measurements of water using the Brillouin lidar technique. Appl. Phys. B *97*, 931–934.

28. Du, D., Darkwa, J., and Kokogiannakis, G. (2013). Thermal management systems for photovoltaics (PV) installations: a critical review. Sol. Energy *97*, 238–254.

29. Fukutani, K., Kanbe, M., Futako, W., Kaplan, B., Kamiya, T., Fortmann, C.M., and Shimizu, I. (1998). Band gap tuning of a-Si:H from 1.55 eV to 2.10 eV by intentionally promoting structural relaxation. Journal of Non-Crystalline Solids *227–230*, 63–67.

30. Baumeister, P.W. (1961). Optical absorption of cuprous oxide. Phys. Rev. *121*, 359–362.

31. Chu, T.L., Chu, S.S., Ferekides, C., and Britt, J. (1992). Films and junctions of cadmium zinc telluride. J. Appl. Phys. *71*, 5635–5640.

32. Wong, T.K.S., Zhuk, S., Masudy-Panah, S., and Dalapati, G.K. (2016). Current status and future prospects of copper oxide heterojunction solar cells. Materials (Basel) *9*, 1–21.

33. Tanaka, T., Yu, K.M., Stone, P.R., Beeman, J.W., Dubon, O.D., Reichertz, L.A., Kao, V.M., Nishio, M., and Walukiewicz, W. (2010). Demonstration of homojunction ZnTe solar cells. J. Appl. Phys. *108*, 024502.

34. Sarswat, P.K., and Free, M.L. (2013). Enhanced photoelectrochemical response from copper antimony zinc sulfide thin films on transparent conducting electrode. Int. J. Photoenergy *2013*, 1–7.

35. El Allali, M., Sorensen, C.B., Veje, E., and Tidemand-Petersson, P. (1993). Experimental determination of the GaAs and Ga1-xAlxAs band-gap energy dependence on temperature and aluminum mole fraction in the direct band-gap region. Phys. Rev., B Condens. Matter. *48*, 4398–4404.

36. Tomasulo, S., Nay Yaung, K., Faucher, J., Vaisman, M., and Lee, M.L. (2014). Metamorphic 2.1–2.2 eV InGaP solar cells on GaP substrates. Appl. Phys. Lett. *104*, 173903.

37. Grassman, T.J., Carlin, A.M., Grandal, J., Ratcliff, C., Yang, L., Mills, M.J., and Ringel, S.A. (2012). Spectrum-optimized Si-based III-V multijunction photovoltaics. Proc. SPIE 8256, Physics, Simulation, and Photonic Engineering of Photovoltaic Devices, Vol. 8256 (International Society for Optics and Photonics), p. 82560R.

38. Miller, O.D., Yablonovitch, E., and Kurtz, S.R. (2012). Strong internal and external luminescence as solar cells approach the Shockley-Queisser limit. IEEE J. Photovoltaics *2*, 303–311.

39. Azzouzi, M., Kirchartz, T., and Nelson, J. (2019). Factors controlling open-circuit voltage losses in organic solar cells. Trends in Chemistry *1*, 49–62.

40. Kaltenbrunner, M., White, M.S., Głowacki, E.D., Sekitani, T., Someya, T., Sariciftci, N.S., and Bauer, S. (2012). Ultrathin and lightweight organic solar cells with high flexibility. Nat. Commun. *3*, 770.

41. Baran, D., Ashraf, R.S., Hanifi, D.A., Abdelsamie, M., Gasparini, N., Röhr, J.A., Holliday, S., Wadsworth, A., Lockett, S., Neophytou, M., et al. (2017). Reducing the efficiency-stability-cost gap of organic photovoltaics with highly efficient and stable small molecule acceptor ternary solar cells. Nat. Mater. *16*, 363–369.

42. Lang, D.V., Chi, X., Siegrist, T., Sergent, A.M., and Ramirez, A.P. (2004). Amorphous like density of gap states in single-crystal pentacene. Phys. Rev. Lett. *93*, 086802.

43. Podzorov, V., and Gershenson, M.E. (2005). Photoinduced charge transfer Across the interface between organic molecular crystals and polymers. Phys. Rev. Lett. *95*, 016602.

44. Pandey, A.K., and Nunzi, J.M. (2007). Upconversion injection in rubrene/perylene-diimide-heterostructure electroluminescent diodes. Appl. Phys. Lett. *90*, 1–4.

45. Voss, K.F., Foster, C.M., Smilowitz, L., Mihailović, D., Askari, S., Srdanov, G., Ni, Z., Shi, S., Heeger, A.J., and Wudl, F. (1991). Substitution effects on bipolarons in alkoxy derivatives of poly(1,4-phenylene-vinylene). Phys. Rev. B *43*, 5109–5118.

46. Hoven, C.V., Yang, R., Garcia, A., Crockett, V., Heeger, A.J., Bazan, G.C., and Nguyen, T.Q. (2008). Electron injection into organic semiconductor devices from high work function cathodes. Proc. Natl. Acad. Sci. USA *105*, 12730–12735.

47. Nielsen, C.B., Holliday, S., Chen, H.Y., Cryer, S.J., and McCulloch, I. (2015). Non-fullerene electron acceptors for use in organic solar cells. Acc. Chem. Res. *48*, 2803–2812.

48. Lee, H.K.H., Telford, A.M., Röhr, J.A., Wyatt, M.F., Rice, B., Wu, J., De Castro Maciel, A., Tuladhar, S.M., Speller, E., McGettrick, J., et al. (2018). The role of fullerenes in the environmental stability of polymer:fullerene solar cells. Energy Environ. Sci. *11*, 417–428.

49. Speller, E.M., Clarke, A.J., Luke, J., Lee, H.K.H., Durrant, J.R., Li, N., Wang, T., Wong, H.C., Kim, J.S., Tsoi, W.C., and Li, Z. (2019). From fullerene acceptors to non-fullerene acceptors: prospects and challenges in the stability of organic solar cells. J. Mater. Chem. A *7*, 23361–23377.

50. Fei, Z., Eisner, F.D., Jiao, X., Azzouzi, M., Röhr, J.A., Han, Y., Shahid, M., Chesman, A.S.R., Easton, C.D., McNeill, C.R., et al. (2018). An alkylated Indacenodithieno[3,2-b] thiophene-based nonfullerene acceptor with high crystallinity exhibiting single junction solar cell efficiencies greater than 13% with low voltage losses. Adv. Mater. *30*, 1705209.

51. Li, S., Ye, L., Zhao, W., Yan, H., Yang, B., Liu, D., Li, W., Ade, H., and Hou, J. (2018). A wide band gap polymer with a deep highest occupied molecular orbital level enables 14.2% efficiency in polymer solar cells. J. Am. Chem. Soc. *140*, 7159–7167.

52. Yuan, J., Zhang, Y., Zhou, L., Zhang, G., Yip, H.-L., Lau, T.-K., Lu, X., Zhu, C., Peng, H., Johnson, P.A., et al. (2019). Single-Junction organic solar cell with over 15% efficiency using fused-ring acceptor with electron-deficient core. Joule *3*, 1140–1151.

53. Rosa-Clot, M., Rosa-Clot, P., Tina, G.M., and Scandura, P.F. (2010). Submerged photovoltaic solar panel: SP2. Renew. Energy *35*, 1862–1865.

54. Zuo, G., Linares, M., Upreti, T., and Kemerink, M. (2019). General rule for the energy of water-induced traps in organic semiconductors. Nat. Mater. *18*, 588–593.

55. Jeong, E.G., Jeon, Y., Cho, S.H., and Choi, K.C. (2019). Textile-based washable polymer solar cells for optoelectronic modules: toward self-powered smart clothing. Energy Environ. Sci. *12*, 1878–1889.